Path Length Correction for Improving Leaf Area Index Measurements Over Sloping Terrains: A Deep Analysis Through Computer Simulation

Gaofei Yin, *Member, IEEE,* Biao Cao, Jing Li, Weiliang Fan, *Member, IEEE,* Yelu Zeng, Baodong Xu, and Wei Zhao, *Member, IEEE*

***Abstract*— The *in situ* measurement of the leaf area index (LAI) from gap fraction is often affected by terrain slope. Path length correction (PLC) is commonly used to mitigate the topographic effect on the LAI measurements. However, the terrain-induced uncertainty and the accuracy improvement of the PLC for LAI measurements have not been systematically analyzed, hindering the establishment of an appropriate protocol for LAI measurements over mountainous regions. In this article, the above knowledge gap was filled using a computer simulation framework, which enables the estimated LAI before and after PLC to be benchmarked against the known and precise model truth. The simulation was achieved by using CANOPIX software and a dedicatedly designed ray-tracing method for continuous and discrete canopies, respectively. Simulations show that the slope distorts the angular pattern of the gap fraction, i.e., increasing the gap fraction in the down-slope direction and reducing it in the up-slope direction. The horizontally equivalent hemispheric gap fraction from the PLC can reconstruct the azimuthally symmetric angular pattern of the real horizontal surface. The azimuthally averaged gap fraction for sloping terrain can both be underestimated or overestimated depending on the LAI and can be successfully corrected through PLC. The topography-induced uncertainty in LAI measurements is found to be ∼14.3% and >20% for continuous and discrete canopies, respectively. This uncertainty can be, respectively, reduced to ∼1.8% and <7.3% after PLC, meeting the up-to-date uncertainty threshold of 15% established by the Global Climate Observing System (GCOS). Closer analysis shows that the topographic effect is influenced by fractional crown cover, and the largest uncertainty which corresponds to extensively clumping canopy can reach nearly up to 50%. The accuracy of the estimated LAI after PLC safely meets the GCOS uncertainty threshold even for this extreme case. This study demonstrates the necessity of a topographic correction for LAI measurements and the applicability of PLC for reconstructing the horizontally equivalent gap fraction and improving the LAI measurements over sloping terrains. The results of this article throw light on the design of a protocol for LAI measurements over mountainous regions.**

***Index Terms*— Computer simulation, *in situ* measurement, leaf area index (LAI), path length correction (PLC), topographic effect.**

I. Introduction

LEAF area index (LAI) is generally defined as one-half of the total area of leaves per unit area of ground [1]. On sloping surfaces, the LAI can be projected to the normal of the slope [2] or to the direction of gravity [3]–[5]. The latter ensures a concordant definition between vegetations growing over horizontal and sloping surfaces, and therefore, is preferable in most of the studies [3]–[5]. The LAI controls the exchanges of energy, water, and greenhouse gases between the land surface and the atmosphere [6]. Therefore, a wide range of surface models used in agriculture, ecology, carbon cycle, climate, and other related studies use LAI as an important input [7].

In situ LAI measurements are indispensable for the calibration of surface models [8] and the validation of remote sensing products [9], [10]. *In situ* LAI measurements can be collected by direct or indirect methods. Direct methods, including destructive sampling and litter collection, are generally seen as the most accurate, but they have the disadvantage of being extremely time-consuming and as a consequence making large-scale implementation only marginally feasible [11]. On the contrary, most of the indirect methods use the gap fraction measurements collected from optical sensors, e.g., LAI-2000 and fisheye lens [12]–[14], and they transfer these measurements to the LAI values based on the Beer's law [11]. Previous studies showed that the indirect methods with proper protocols can achieve equivalent or even better accuracy than direct methods [15]–[17]. In recent years, more

Manuscript received July 16, 2019; revised October 24, 2019; accepted December 23, 2019. Date of publication January 30, 2020; date of current version June 24, 2020. This work was supported in part by the National Natural Science Foundation of China under Grant 41531174, Grant 41971282, Grant 41601403, and Grant 41601478, in part by the GF6 Project under Grant 30-Y20A03-9003-17/18, and in part by the Youth Innovation Promotion Association CAS under Grant 2016333. *(Corresponding author: Wei Zhao.)*

Gaofei Yin is with the Faculty of Geosciences and Environmental Engineering, Southwest Jiaotong University, Chengdu 610031, China (e-mail: yingf@swjtu.edu.cn).

Biao Cao and Jing Li are with the State Key Laboratory of Remote Sensing Science, Institute of Remote Sensing and Digital Earth, Chinese Academy of Sciences, Beijing 100101, China.

Weiliang Fan is with the School of Environmental and Resources Science, Zhejiang A & F University, Lin'an 311300, China.

Yelu Zeng is with the Department of Global Ecology, Carnegie Institution for Science, Stanford, CA 94305 USA.

Baodong Xu is with the Macro Agriculture Research Institute, College of Resource and Environment, Huazhong Agricultural University, Wuhan 430070, China.

Wei Zhao is with the Institute of Mountain Hazards and Environment, Chinese Academy Sciences, Chengdu 610010, China, and also with the Key Laboratory of Geospatial Technology for Middle and Lower Yellow River Regions, Henan University, Ministry of Education, Kaifeng 475004, China (e-mail: zhaow@imde.ac.cn).

Color versions of one or more of the figures in this article are available online at http://ieeexplore.ieee.org.

Digital Object Identifier 10.1109/TGRS.2019.2963366

portable or even fully automatic observation instruments, such as LAINet [18]–[20], LED sensors [21], PASTIS-57 [22], and smartphones [23], [24], have emerged. The indirect methods are more and more operational and preferred because of their improved accuracy and portability.

It has been well recognized that topography modifies the canopy structure and thereby distorts the angular distribution of the gap fraction [25]–[27]. Without considering this effect, the topography-induced uncertainty embedded in the gap fraction measurements will propagate to the final LAI estimations and reduce the estimation accuracy, especially for the dense canopies and/or steep slopes [3], [5]. Therefore, several methods were proposed to address the topographic effect in *in situ* LAI estimation. To the best of our knowledge, Frazer *et al*. [28] were the first trying to address the topographic effect in LAI estimation from optical measurements. In their proposed method, the sensor was tilted along the slope's normal rather than the vertical direction, reducing the variation of the gap fraction with the azimuth. However, it is hard to fix the sensor to this special direction during the field campaign, so this method was seldom used in practice. Schleppi *et al*. [5] proposed an iterative method to mitigate the azimuthal dependence of the gap fraction caused by a slope, yet this method is without analytical formulation for the topographic correction.

Path length, defined as the distance the light travels through the canopy, is a critical variable influencing the radiative transfer process and is related to the canopy structure [29], [30]. The slope significantly distorts the angular distribution of path length. For example, relative to the horizontal terrain, surface topography compresses the path length in the downslope direction and stretches it in the up-slope direction [3]. Therefore, several studies employ path length correction (PLC) to reduce the topographic effect in LAI measurements [3], [4], [27], [31]. The key difference existed in these PLC-based LAI measurement methods lies in how to formulate the path length for sloping surfaces: Walter and Torquebiau [27] and Duursma *et al.* [31] used local incidence angle, instead of the zenith angle itself, to calculate the path length; Montes *et al.* [4] computed the path length by adding the local slope angle to zenith angle; and Luisa *et al.* [3] proposed a path length formula based on rigorous trigonometric consideration. All of the above three methods are very simple to implement and have the potential to reduce the topographic effect on LAI measurements, yet the method proposed by Luisa *et al.* [3] is more preferred in recent studies because it maintains the geotropic nature of vegetation growth and the azimuthal symmetry assumption of the leaf inclination distribution function [3], [30], [32]. The completeness in mechanism gives it another advantage over the other methods, i.e., it can reconstruct horizontally equivalent gap fraction for sloping canopies [3]. With this horizontally equivalent gap fraction data in hand, the LAI estimation procedure for the horizontal surface can be safely used subsequently without explicitly considering the topographic effect again. This treatment makes the existing LAI estimation algorithms and software, e.g., CAN_EYE [16] and CIMES [33], usable even for sloping surfaces.

The PLC method has achieved its popularity in *in situ* LAI measurement [3], [4], [27], [31] and even other research fields including clumping index estimation [29], [34], canopy reflectance modeling [30], and topographic normalization for remote sensing imaginary [32]. However, the accuracy of the PLC *per se* has not undergone critical assessment because of the lack of groundtruth data. For example, a previous study [3] found that PLC generally decreases the retrieved LAI for discrete canopies, yet the rationality of this decrease and the absolute accuracy of the improved retrieval procedure could not be given without the groundtruth.

Computer simulation is an efficient alternative for validation activities [35], [36]. It provides a highly controlled environment to implement the validation, and all the disturbing factors influencing the LAI estimation (including leaf orientation, clumping, and woody materials) can explicitly be specified. Moreover, it can cover various conditions existed in the real world through dedicatedly designed scenarios, increasing the representativeness of the validation results. Through computer simulation, Luisa *et al.* [3] found that PLC can improve the accuracy of LAI retrieval, and Cao *et al.* [25] compared five slope correction methods for LAI estimation and demonstrated that the PLC method outperformed the other existing methods. However, during their computer simulations, the PLC was assessed only for continuous canopies and the performance of the PLC method for discrete canopies is still unknown. In addition, only the final accuracies were given, and the intermediate products (e.g., horizontally equivalent gap fraction) of PLC were not analyzed.

The objective of this study is to critically assess the performance of PLC for improving LAI measurements over sloping terrains. A deep analysis through computer simulation will be implemented to fulfill this objective. This study addresses three main specific questions concerning PLC.

1) Is the computer simulation an effective tool in the assessment of PLC for the topographic effect suppression?
2) Can the PLC method provide realistic intermediate variables of the LAI estimation process (e.g., horizontally equivalent gap fraction and azimuthally averaged gap fraction)?
3) How does the PLC method, deduced from continuous canopy assumption, perform for discrete canopies?

This article will be organized as follows. Section II provides the background theory for LAI estimation and PLC. Then, the computer simulation method and scenario designed for continuous and discrete canopies will be provided in Section III. The assessment results for the PLC will be described in Section IV. Finally, discussion and conclusion are presented in Sections V and VI, respectively.

II. Theory Background

A. Beer's Law for LAI Estimation

Indirect methods generally retrieve LAI from the gap fraction measurement by inverting the Beer's law

$$P(\theta, \varphi) = e^{-G(\theta)\rho l(\theta,\varphi)} \tag{1}$$

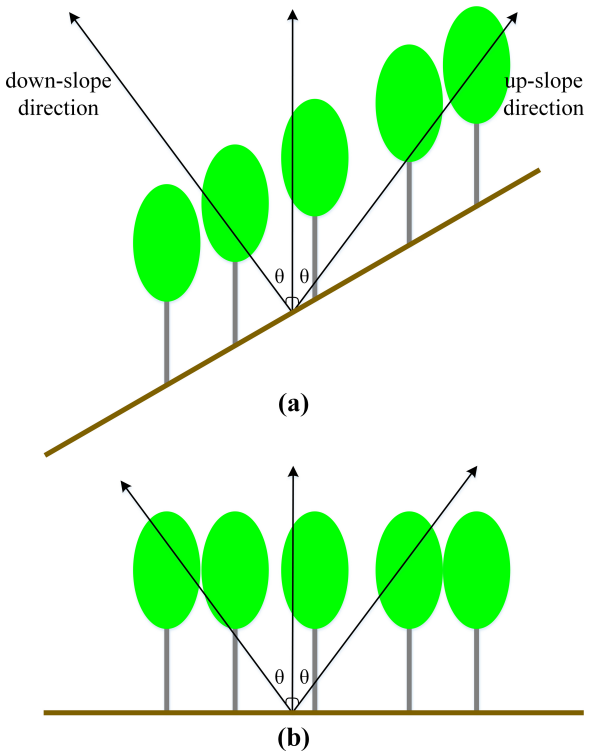

Fig. 1. Schematics of path length over (a) sloping and (b) horizontal surfaces. The two plots are with the same canopy structure but different path lengths because of different surface orientations.

where θ and φ are the zenith and azimuthal angles, respectively; P is the gap fraction; G, referred to as the projection function, is the area of a unit LAI projected along the direction (θ, φ) and is often assumed to be azimuthally symmetrical; ρ is the leaf area volume density (m^2/m^3); l is the path length, i.e., the distance the light travels through the canopy. LAI can be calculated as the product of ρ and the path length in nadir direction.

Equation (1) assumes that the leaves are randomly distributed within the canopy. For discrete canopies, this study assumed a horizontally continuous distribution of leaves within crowns. Small canopy gaps within the crowns and the larger canopy gaps between crowns exist for discrete canopies. No attenuation will occur when light passes through the between-crown gaps, and the transfer of radiation within crown obeys Beer's law. In fact, the clumping index can be introduced to account for the leaf clumping phenomenon [37], [38], which is out of the scope of this study.

B. PLC for Sloping Terrains

For a continuous canopy over flat terrain, the path length is independent of azimuthal angle which can be simply computed as follows:

$$l(\theta) = 1/\cos(\theta). \tag{2}$$

Over a sloping surface, plants are still geotropic, i.e., the topography may not influence the architecture of individual plants too much. However, topography extremely influences the topological relationship between different plants [39], and then the path length within the canopy is distorted [30], [32]. An illustration of how topography affects the path length can be seen in Fig. 1. Compared with a horizontal surface, topography stretches the path length in the up-slope direction and compresses it in the down-slope direction. For a horizontal surface, the minimal path length is in the nadir direction, and the value of the path length in this direction is not impacted by topography because of the geotropic nature of vegetation growth. However, the minimal path length changes with slope. For the sloping surface, the minimal appears in the direction normal to the surface.

By applying trigonometric relationships, Luisa *et al.* [3] deduced the following path length expression for sloping surface:

$$l(\theta, \varphi, \alpha, \beta) = \frac{1}{\cos\theta(1 - \tan\alpha\cos(\varphi - \beta)\tan\theta)} \tag{3}$$

where θ and φ are the same as in (1). α and β are the slope and aspect of the sloping surface, respectively.

Equations (2) and (3) both can be substituted into (1) and obtain the gap fraction for horizontal and sloping surfaces with identical canopy parameters. Therefore, a simple transformation from the gap fraction for the sloping surface to that for a horizontal surface can be identified as follows [3]:

$$P_f = (P_s)^{\lambda} \tag{4}$$

where P_s is the gap fraction for the sloping surface; P_f is the gap fraction for a hypothetical horizontal surface with identical canopy parameters as the sloping surface, referred to as horizontally equivalent gap fraction in the following; the transformation factor, λ, is expressed as follows:

$$\lambda = 1 - \tan\alpha\cos(\varphi - \beta)\tan\theta. \tag{5}$$

The parameters in (5) have the same meaning as in (3).

The PLC method can reconstruct the horizontally equivalent gap fraction for sloping surface measurements given the topographic factors (slope and aspect) in a very simple way [see (4)]. LAI can be retrieved from horizontally equivalent gap fraction data using existing algorithms and software designed for a horizontal surface, making the LAI estimation over sloping surfaces simple and flexible.

III. Materials and Methods

Our main aim is to develop a simulation framework to assess the PLC method designed for improving LAI estimations over sloping surfaces. The assessment will be implemented for continuous and discrete canopies, respectively, under dedicatedly designed canopy parameters. The simulation consists of four main steps: 1) simulating hemispherical gap fraction for horizontal and sloping surfaces; 2) reconstructing horizontally equivalent gap fraction for sloping surfaces; 3) calculating azimuthally averaged gap fraction; and 4) estimating LAI from azimuthally averaged gap fraction using the lookup table (LUT) method and assessing the performance of PLC. The simulation of hemispherical gap fraction is the key to this study and is achieved using CANOPIX software [5] and the ray-tracing method for continuous and discrete canopies, respectively.

TABLE I
SPECIFICATIONS OF THE LAI, LEAF ANGLE INCLINATION (ALA), AND SLOPE USED TO SIMULATE HEMISPHERICAL GAP FRACTION OF CONTINUOUS CANOPY FROM CANOPIX

Parameter	Specification
LAI	1, 2, 3, 4, 5.
ALA	27°, 57°, 63°.
Slope	0°, 10°, 20°, 30°, 40°, 50°.

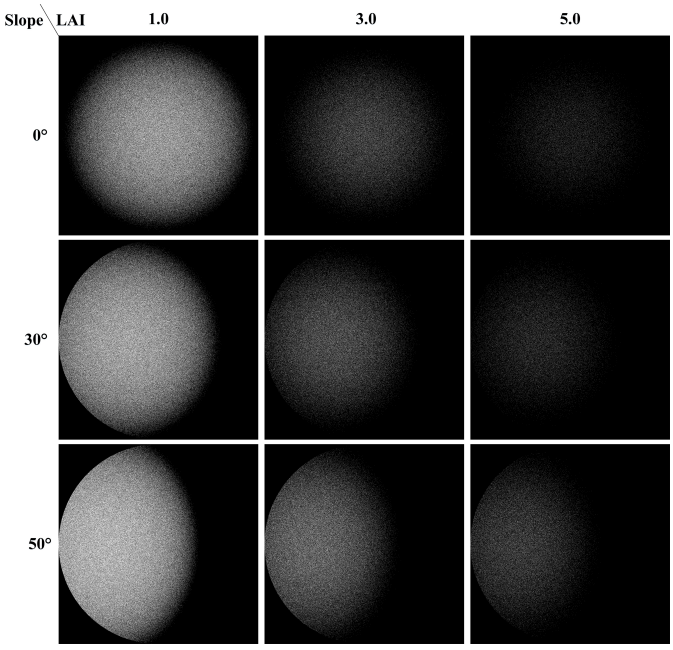

Fig. 2. Examples of simulated hemispherical photographs for continuous canopies with LAI values of 1, 3, and 5, slope values of 0°, 30°, and 50°, and spherical leaf inclination angle distribution.

A. Simulating Hemispherical Gap Fraction for Continuous Canopy

CANOPIX [5] can produce artificial canopy hemispherical photography (HP) according to three user-set parameters: LAI, average leaf angle inclination (ALA), and ground slope. LAI in our simulation ranges from 1 to 5 with a step of 1; the three typical leaf inclination angle distributions, i.e., planophile, spherical, and erectophile with ALA of 27°, 57°, and 63°, respectively, were selected as recommended by Leblanc and Fournier [35]; the slope was set from 0° to 50° with a step of 10°, to simulate flat to extremely steep slopes. Specifications of the input for CANOPIX simulations can be found in Table I.

Examples of simulated HPs are shown in Fig. 2. The white pixels in the simulated HPs present gaps within the homogenous canopy. To calculate the hemispherical gap fraction, the simulated HPs were divided into equiangular annuli and azimuthal sectors (see Fig. 3). In this study, the widths of the zenith annuli and azimuthal sector were set to 5° and 15°, respectively. The gap fraction in each segment can be easily calculated as the ratio between the numbers of the white and total pixels.

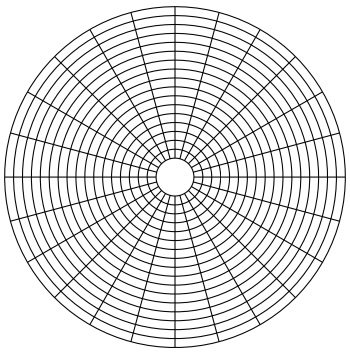

Fig. 3. Hemispherical segments for gap fraction calculation.

B. Simulating Hemispherical Gap Fraction for Discrete Canopy

The simulation of the hemispherical gap fraction for discrete canopies consists of three main steps: 1) three virtual scenes over horizontal surface represent sparse, medium, and dense forests were first generated; 2) the path lengths of photons (along the different directions) within tree envelopes were then simulated by ray tracing. Before ray tracing, the horizontal surface was rotated (maintaining the geotropic nature of vegetation growth) to simulate path lengths for sloping surfaces; and 3) gap fraction was calculated using Beer's law [see (1)] given the simulated path length of step (2), projection function, and leaf area volume density.

1) Design of Virtual Scenes: The simulation was constrained in a 100 m × 100 m area, corresponding to a forest stand. The tree envelope was abstracted as a spheroid with crown width and length of 5 and 10 m, respectively. The influence of leaf clumping around branches and twigs was neglected, and leaves were assumed to be randomly distributed within the crown envelope. The trees were randomly located, nevertheless, too much overlapping between tress was not allowed to account for plant competition. This was achieved by setting a minimal exclusion distance (4.0 m) [40], and if the distance between two trees was less than the exclusion distance, one of them was deleted and put to a new location. This implementation was iterated until distances between any two trees were all larger than the exclusion distance. Three virtual scenes, with a tree number of 200, 300, and 400, were generated to represent sparse, medium, and dense forests (see Fig. 4). The fractional crown covers (FCCs) for the three scenes were 39%, 57%, and 74%, respectively.

The sloping forests were generated by rotating the bottom plane of the horizontal scenes, and the geotropic nature of vegetation growth is reserved during the rotation process. The bottom plane was rotated from 0° to 50° with a step of 10°, consistent with the continuous settings (see Table I).

2) Ray Tracing for Path Length Simulation: The path length was simulated by ray tracing. The upper boundary of the scene is divided into grids with a side length of 0.5 m, and the photons were originally placed on the grid points. The paths of individual photons along a direction are traced from

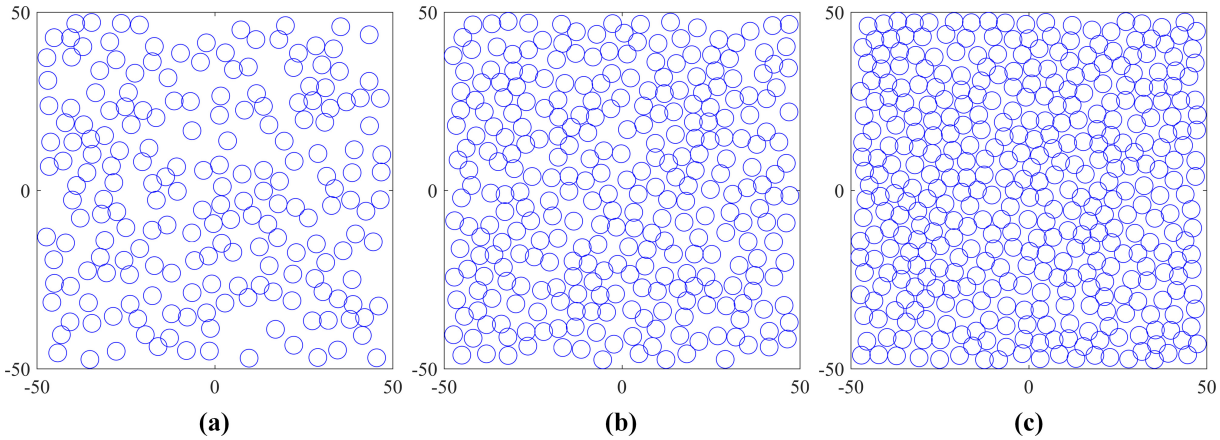

Fig. 4. Horizontal distribution of trees for the virtual scenes. The FCCs were (a) 39%, (b) 57%, and (c) 74%, respectively.

their origins until they hit the bottom boundary. Photons may traverse more than one tree, and the accumulated geometric distance within crown envelopes is seen as the path length. If no tree has collided, the path length was set to zero. The spatial distribution of the path length can be generated by this method.

The ray-tracing procedure can be summarized as follows.

1) A photon is initialized at a grid point in the upper boundary.
2) The nearest point ($\vec{r}$) of the intersection of the photon along a direction Ω with a tree is found.
3) Calculate and record the geometric distance of the photon traversing within the current crown (l_i).
4) Locate the photon to a new position $\vec{r} = \vec{r} + l_i\Omega$ and find the next collision position along Ω.
5) If the next collision position is located on a crown envelope, repeat from step (3). Otherwise (the next collision occurs on the bottom boundary), accumulate l_i and assign it to the grid point as the path length there.
6) Repeat from step (1), for each grid point in the upper boundary.

To improve the efficiency in searching for the intersection points, the definition of "view factors" $v(i, j)$ for each pair of trees i and j is introduced [41]. The view factors define the angular range of directions from tree i which may intersect tree j. They are calculated and tabulated before ray tracing. During ray tracing, only trees included in the range of view factors for a tree was considered. In addition, if photons go out the boundary of the scene, they make a reentry on the opposite side of the scene, to avoid the side effect.

The ray-tracing algorithm proposed in this section can give a detailed spatial distribution of the path lengths for the virtual scenes. Examples for the dense forest stand [Fig. 4(c)] under different topographies are shown in Fig. 5. These images represent the spatial distribution of the path length with 0.5-m resolution. Although, they were simulated for the same observation angle (30°) and scene [Fig. 4(c)], the prominent discrepancy can be obviously observed, revealing a significant influence of topography on path length distribution within canopy: relative to the horizontal case, the path lengths in the up-slope [Fig. 5(b)] and down-slope [Fig. 5(d)] directions are significantly stretched and squeezed by topography, respectively. It is worth noting that when the aspect of the sloping surface is perpendicular to the observation direction, the slope exerts a negligible influence on the path length. This interesting phenomenon can be clearly observed in Fig. 5(c): the distribution of path lengths in this special direction (mean path length = 5.87 m) is very similar to the horizontal case (mean path length = 5.83 m).

TABLE II
SPECIFICATIONS OF PARAMETERS USED TO SIMULATE HEMISPHERICAL GAP FRACTION OF DISCRETE CANOPY FROM RAY TRACING

Parameter	Specification
Crown height	10 m.
Crown width	5 m.
Tree number	200, 300, 400.
LAI	1, 2, 3, 4, 5.
ALA	27°, 57°, 63°.
Slope	0°, 10°, 20°, 30°, 40°, 50°.

3) Hemispherical Gap Fraction Calculation: Using the procedure of ray tracing, path lengths in different directions (see Fig. 3) under different combinations of slopes and tree numbers can be tabulated in advance. Assuming leaves are randomly distributed within the crown, Beer's law can be safely used to estimate the gap fraction given LAI and ALA. To obtain the aggregate gap fraction for the stand, the gap fraction at each pixel was calculated and averaged. The alternative for this procedure, i.e., first averaging the path length over the stand and calculating the aggregate gap fraction from the averaged path length directly, will incur scale effects [42], and therefore was not adopted.

The parameter specifications for discrete canopies simulation is summarized in Table II.

C. LAI Estimation

Azimuthally averaged gap fraction, the input for most of the LAI estimation algorithms [7], was calculated by the simulated

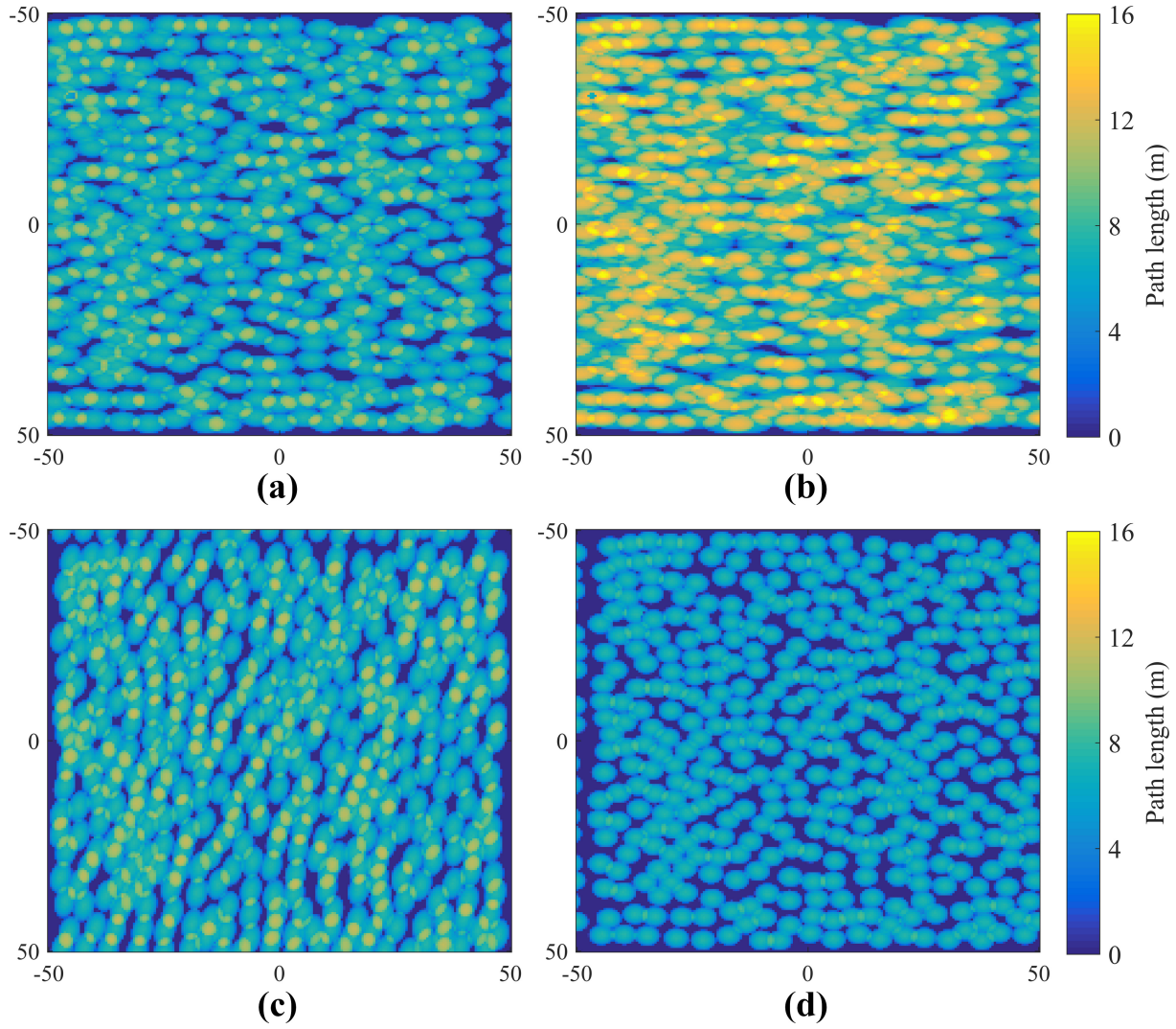

Fig. 5. Spatial distribution of path length within the virtual dense forest (with FCC of 74%). The observation zenith and azimuth angles were all set as 30° and 0°, respectively. The slopes and aspects of the sloping surfaces were (a) 0° and 0°, (b) 30° and 0°, (c) 30° and 90°, and (d) 30° and 180°. The mean path lengths of the four simulations were 5.83, 8.81, 5.87, and 4.40 m, respectively.

hemispherical gap fraction. The topographic mask, up-slope areas blocked by sloping surface, was masked out before computing the azimuthally average gap fraction, in accordance with the existing protocol of LAI estimation for rugged terrains [3], [26].

The LUT method was used to estimate the LAI from the azimuthally averaged gap fraction. LUT records the LAI and the corresponding gap fraction in multiple zenith angles. Too large zenith was commonly not used in reality to avoid the influence of diffuse scattering and mixed pixels for digital HP [43]. The zenith angles were, therefore, set from nadir to 62.5° with a step of 5°.

Four LUTs were constructed for continuous canopy, sparse, medium, and dense discrete canopy, respectively. For the continuous canopy LUT, the multiangular gap fraction was calculated using (1) and (2). The multiangular gap fraction for the three forest scenes was yet simulated by ray tracing (for horizontal surfaces) to account for their obvious clumping characteristics. The four LUTs have the same combinations of LAI (ranging from 0.1 to 6 by 0.1 step) and ALA (ranging from 20 to 70° by 2° step). We acknowledge that the respective use of LUTs for different canopies may be too ideal for real-field LAI measurements. However, this treatment can reduce the ill-condition of the inverse problem, and specifically analyze the uncertainty incurred by topography. When estimating the LAI, the simulated gap fraction was compared with those stored in the LUT. The ten best items that can minimize gap fraction difference in terms of root-mean-square error (RMSE) were recorded as acceptable solutions, and their average of LAI is the final estimate value. This "multisolution" method is a commonly used treatment to account for the ill-posed problem [44].

To assess the LAI estimation improvement caused by PLC, we constructed LUTs only for the horizontal surface. The accuracy of the estimated LAI using the corresponding horizontal LUT before and after PLC will be compared. To quantify the retrieval performance, three indicators were adopted, i.e., the coefficient of determination (R^2), relative root-mean-square error (R-RMSE), and relative bias (R-Bias) to assess the goodness of fit, general accuracy, and system

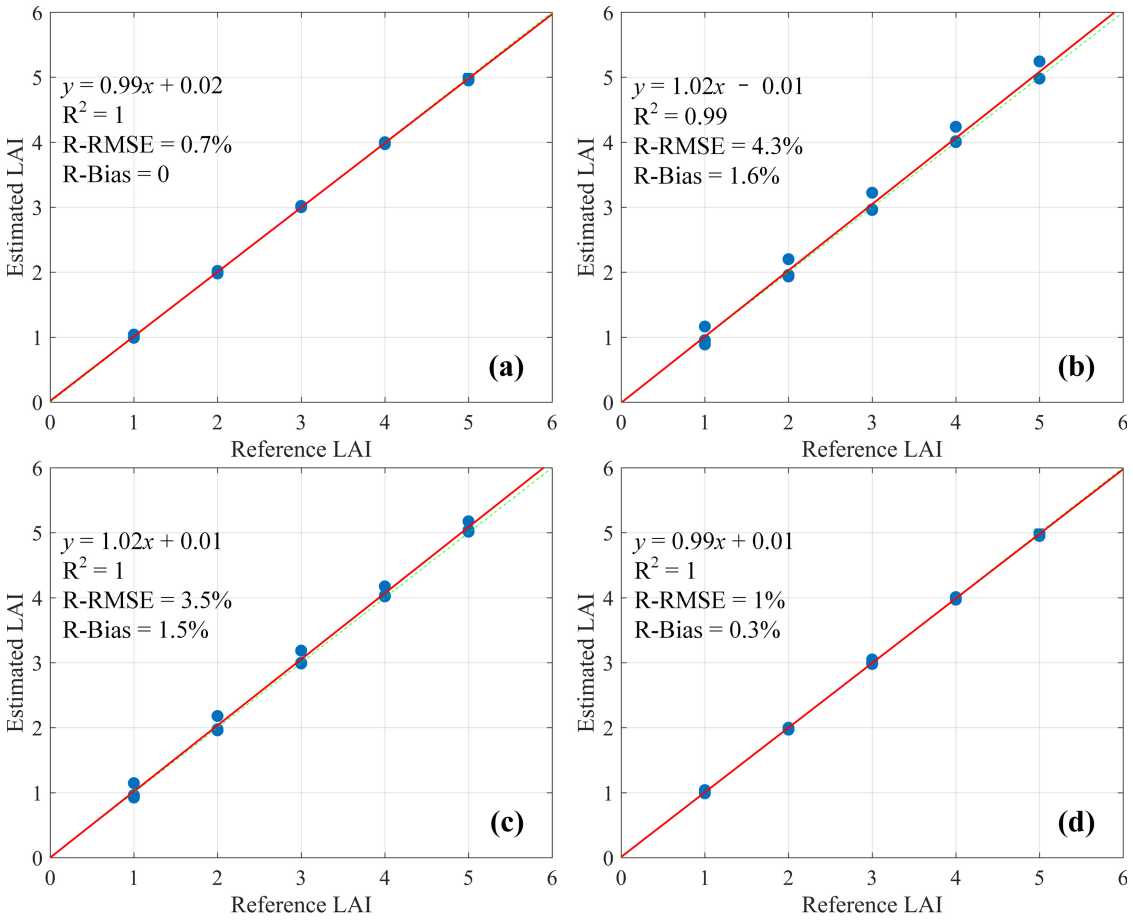

Fig. 6. Comparisons of the reference LAI with LUT-estimated LAI. The canopies are assumed to be (a) continuous and discrete with FCCs of (b) 39%, (c) 57%, and (d) 74%, respectively.

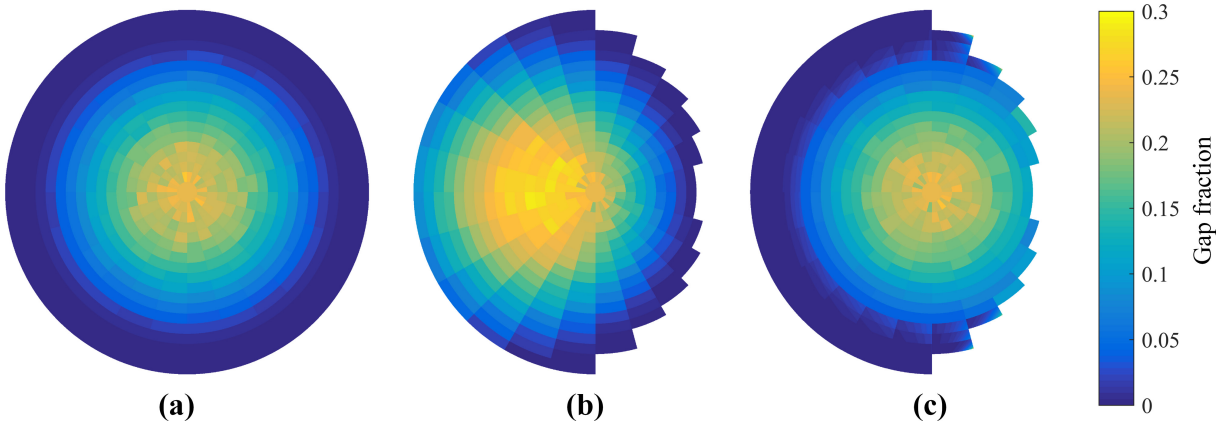

Fig. 7. Gap fraction over the (a) horizontal surface and a 30° sloping surface (b) before and (c) after PLC. The simulated gap fraction is under the same canopy structure, i.e., LAI of 3.0 and spherical leaf inclination angle distribution. The canopies are assumed to be continuous during the simulation.

bias, respectively. R-RMSE and R-Bias were defined as the RMSE and Bias normalized by the average of reference values, i.e., the inputs of the computer simulation. The uncertainty caused by the retrieval process *per se* is slight, with R^2 nearly equals 1.0, R-RMSE and R-Bias less than 4.3% and 1.6%, respectively (see Fig. 6). The good performance of the LUT method for horizontal surfaces can make us neglect the uncertainty caused by the estimation process and focus on topographic effect and correction.

IV. Results

A. Continuous Canopies

1) Topographic Correction of Gap Fraction: Fig. 7 shows CANOPIX [5] simulated hemispherical gap fraction for a continuous canopy with an LAI of 3.0 and spherical leaf inclination angle distribution. For better comparison, the gap fraction over the horizontal surface [Fig. 7(a)], a 30° sloping surface before [Fig. 7(b)] and after PLC [Fig. 7(c)] are all

shown. The gap fraction for the horizontal surface exhibited azimuthal symmetry and decreased with a zenith angle with the maximum value located in the nadir direction. The slope distorted the angular pattern of the gap fraction. Generally, slope exaggerated the gap fraction in the down-slope direction, and diminished it in the up-slope direction [the right part in Fig. 7(b)]. The maximum gap fraction was also shifted from the nadir to the normal to the surface. After PLC, the original gap fraction for the horizontal surface was satisfactorily restored both in magnitude and angular pattern except that topographic mask could not be retrieved because of surface occlusion.

The azimuthally averaged gap fraction corresponding to Fig. 7 was also analyzed. For a more comprehensive understanding of the topographic effect for different LAI values, we added the cases for LAI of 1.0 and 5.0 (Fig. 8). For a small zenith ($<30°$), the gap fraction over the sloping surface was very similar to the horizontal case, and the discrepancy between the horizontal and sloping gap fraction gradually increased with zenith. For a small LAI case [e.g., LAI $= 1$ as in Fig. 8(a)], the gap fraction over the sloping surface was lower than the horizontal case for most of the zeniths. The exception appeared when the zenith was extremely slant, e.g., zenith $= 62.5°$. On the other hand, for a large LAI [e.g., LAI $= 5$ as in Fig. 8(c)], the gap fraction over the sloping surface was always larger than the horizontal case. The canopy with a medium LAI was independent of terrain when the observation zenith was not too large, and the gap fraction for sloping surface and horizontal surface nearly coincided with each other when the zenith was less than 50°. The PLC method performed very well, and the corrected azimuthally gap fraction was nearly the same as that for the corresponding horizontal surface.

2) LAI Estimation: Simulation found that the slope significantly influences the LAI retrieval accuracy, and the uncertainty caused by topographic effects is about 14.3% (quantified by R-RMSE) for continuous canopies [Fig. 9(a)]. The estimated LAI was overestimated and underestimated for small (e.g., LAI $= 1.0$) and larger LAI (>2.0), respectively, without the consideration of the topographic effect. When LAI is 2.0, there is no obvious bias observed. Generally, the topographic effect caused underestimation of the LAI with R-Bias of -4.6%. After PLC, the consistency between estimated and reference LAI was significantly improved [Fig. 9(b)]: most of the points clustered around the 1:1 line ($R^2 = 1$); R-RMSE was reduced to 1.8% without any obvious bias (R-Bias $= 0.3\%$).

To further investigate the influence of slope on LAI estimation and the dependence of the topographic effect on the LAI value, we analyzed the change of R-RMSE with slope and LAI (Fig. 10). Without considering the topographic effect, the R-RMSE increased gradually from less than 3% (for a slope of 10°) to nearly 25% (for a slope of 50°). LAI *per se* also influences the magnitude of the topographic effect. When LAI is 2.0, the estimated LAI shows the least sensitivity to slope because the increase of the gap fraction in the down-slope direction compensates the decrease in the up-slope direction. The PLC method is very stable and robust with respect to different slopes and LAIs.

B. Discrete Canopies

1) Topographic Correction of Gap Fraction: The simulated hemispheric and azimuthally averaged gap fraction for a discrete canopy with FCC of 74% before and after PLC, and the corresponding horizontal cases are shown in Figs. 11 and 12. Besides canopy representation (continuous versus discrete), other factors, including LAI, ALA, and slope, were all set as the same as in Figs. 7 and 8. Very similar topography-induced distortion of the gap fraction angular distribution can be observed with a difference in magnitude. The sloping gap fraction after PLC exhibits a high degree of consistency with the corresponding horizontal gap fraction: demonstrating the good applicability of PLC even for discrete canopy in reconstructing the horizontally equivalent gap fraction.

2) LAI Estimation: The scatter plots between the reference and LUT estimated LAI before and after PLC for the three virtual scenes (see Fig. 4) are shown in Fig. 13. For the sparse forest, slope incurred both overestimation and underestimation. The estimated LAI was overestimated for small and medium slopes ($\leq 30°$), and overestimated for steep slopes ($>30°$). For medium and dense forests, the estimated LAI was generally underestimated. Generally, the slope-caused uncertainty in forest LAI measurement is more than 20%, and is impacted by FCC: a sparser forest with more clumping is more sensitive to slope and vice versa. With the increase of FCC, the pattern of the scattering plot becomes more similar to that for continuous canopies [see Fig. 9(a)]. After PLC, the LAI estimation accuracy is significantly improved (the right column of Fig. 13). Although slight underestimation can also be observed after PLC, the R^2 (representing goodness of fit) was increased to nearly 1.0, and the R-RMSE (representing general accuracy) was less than 7.3%. What is more, PLC performs stably and robustly even for sparse forest.

Variation of LAI estimation uncertainty (represented by R-RMSE) for forest with slope and LAI is shown in Fig. 14. R-RMSE gradually increased to around 15% with slope when the slope was less than 30°, then the increase was accelerated and even to about 50% for the sparse forest. After PLC, the R-RMSEs for the three forest scenes were all less than 15% even for the steepest slope (50°). The magnitude of the topographic effect was also influenced by the LAI value. The larger LAI incurred a strong topographic effect and vice versa. The PLC method was robust with respect to slope and LAI.

V. Discussion

A. Topographic Effect on LAI Measurement

High accuracy LAI measurements are the prerequisite for surface model calibration and remote sensing product validation [45]. The uncertainty comes from many factors, including illumination condition, canopy clumping, and sampling strategy [46]. The topography-induced uncertainty for LAI measurement is worth being quantified because a significant proportion of vegetation grows in mountainous regions.

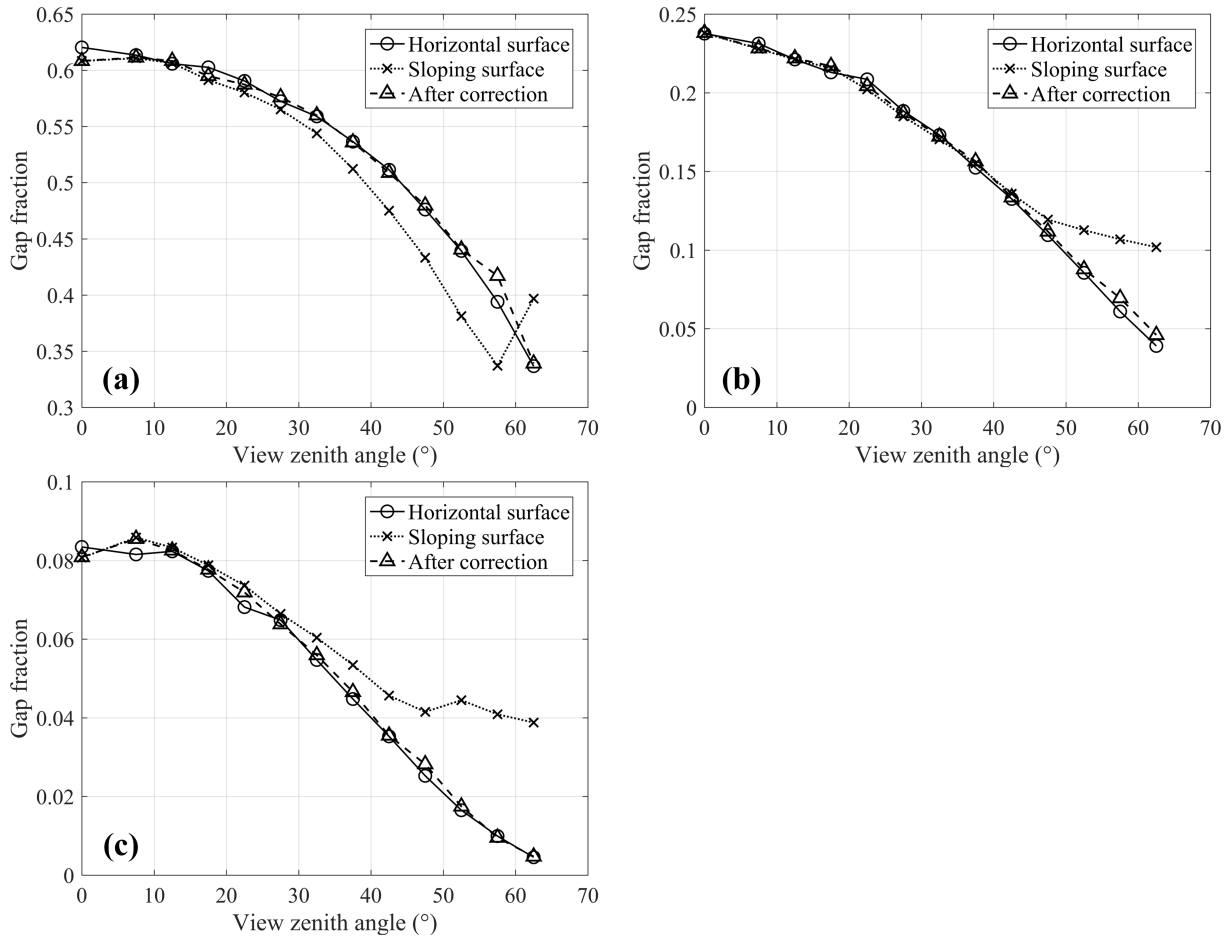

Fig. 8. Azimuthally averaged gap fraction versus view zenith angle for continuous canopies. The leaf inclination angle distribution was spherical, and the slope was set as 30° for sloping surface. LAIs were set as (a) 1.0, (b) 3.0, and (c) 5.0, respectively.

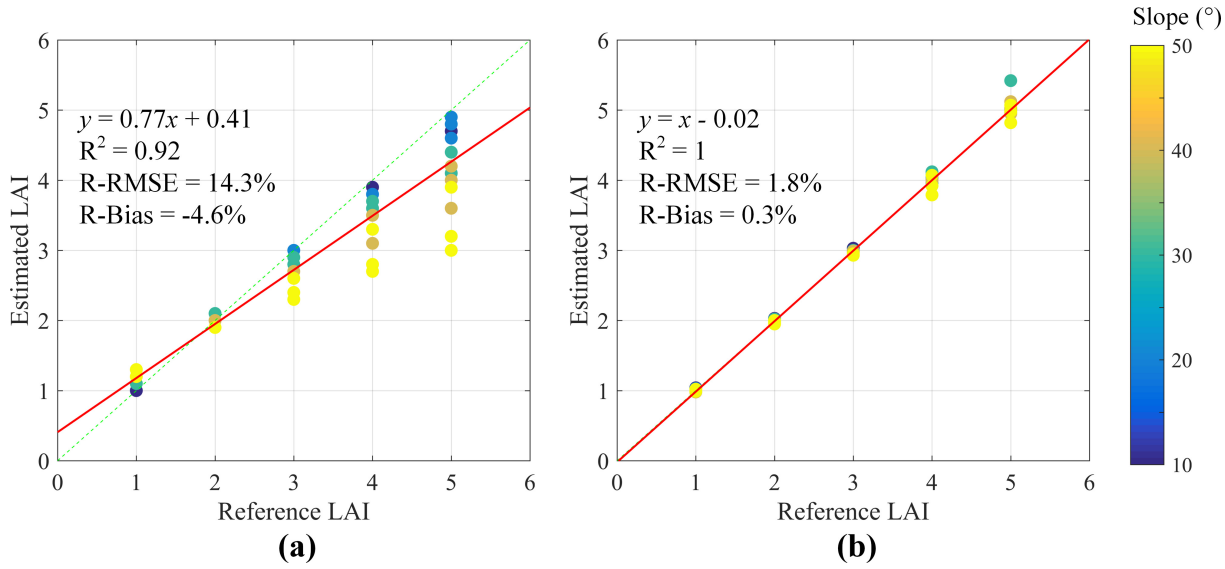

Fig. 9. Comparisons of the reference LAI with estimated LAI (a) before and (b) after PLC. The canopies are assumed to be continuous and overlaid sloping surfaces during the simulation.

Several studies focusing on the topography effect on LAI measurement and its correction exist in the literature [3], [5], [25]–[27], and [31]. The topography-induced uncertainty has not been explicitly quantified because of the lack of sufficient *in situ* measurements over mountainous regions. This study quantitatively analyzed the topography-induced uncertainty by an alternative way: computer simulation. Results show that the uncertainty caused by the

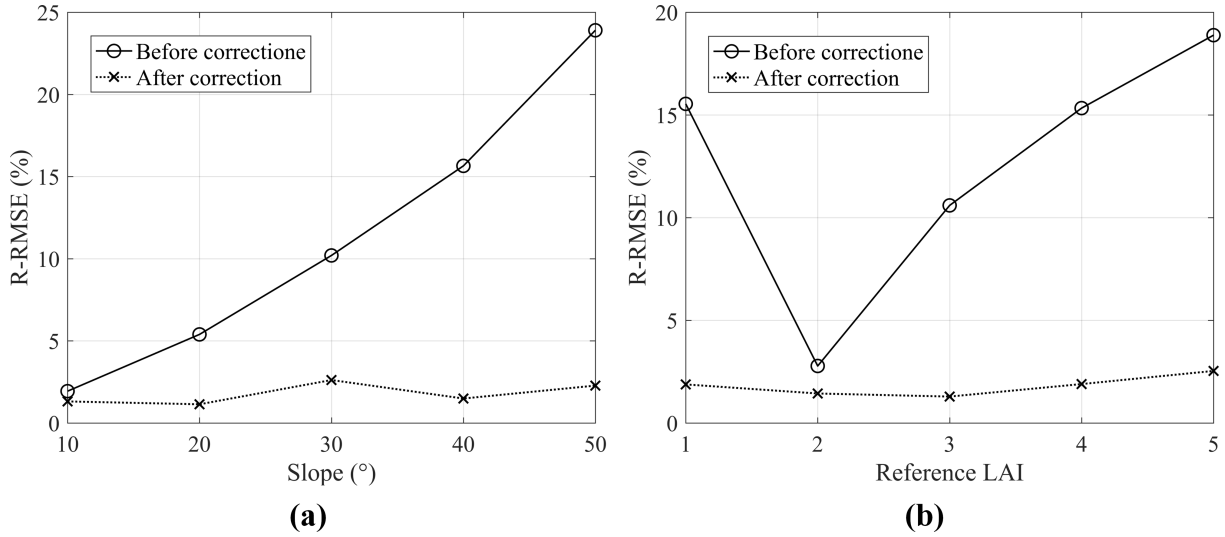

Fig. 10. Variation of LAI estimation uncertainty (represented by R-RMSE) with (a) slope and (b) reference LAI for continuous canopy.

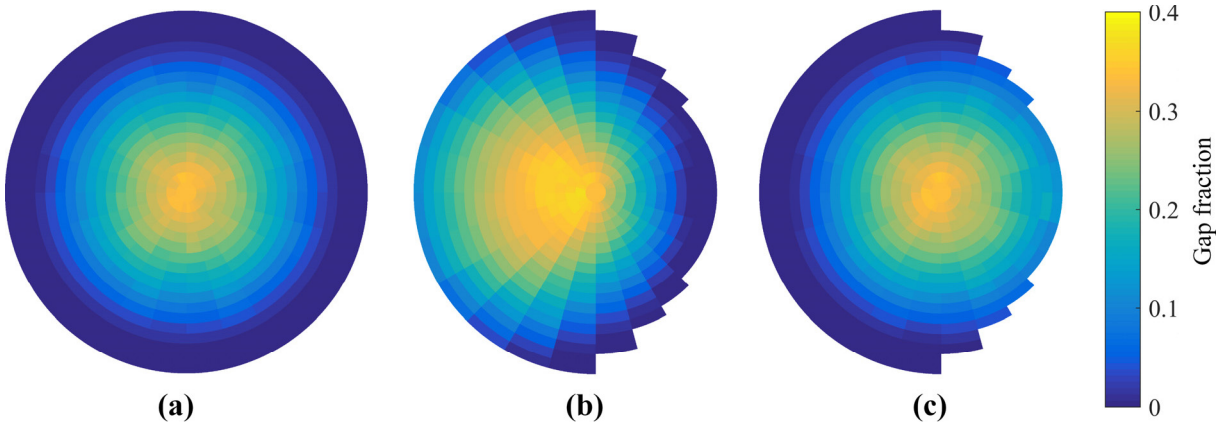

Fig. 11. Gap fraction over the (a) horizontal surface and a 30° sloping surface (b) before and (c) after PLC. The hemispherical gap fraction is under the same canopy structure, i.e., LAI of 3.0 and spherical leaf inclination angle distribution. The canopy is assumed to be a dense forest with FCC of 74%.

topographic effect for LAI measurement is about 14.3% and more than 20% (quantified by R-RMSE) for continuous and discrete canopies, respectively. The R-RMSE can be analyzed against the up-to-date uncertainty threshold (15%) proposed by the Global Climate Observing System (GCOS) [47]. The topography-induced uncertainty alone approaches or even surpasses this threshold. Considering other uncertainty attached to commonly used optical instruments and estimation algorithms (ranging from 10% to 20%, depending on operating environments [48]–[50]), topographic correction should be explicitly used before LAI estimation over mountainous regions.

Discrete canopy is more sensitive to topography effect than the continuous canopy. The magnitude of topography-induced uncertainty depends on several factors. The largest uncertainty corresponds to a canopy with large LAI and sparse FCC over a steep slope and can reach nearly 50% (see Fig. 14).

In this study, the topography-induced uncertainty was found dominant by underestimation, consistent with existing studies [3], [5], [25]. However, overestimation also occasionally happens. Two factors determine the compromise between the overestimation and the underestimation: 1) the tradeoff between the path length reduction in the down-slope direction and stretch in the up-slope direction and 2) the nonlinear relationship between the gap fraction and path length given projection function and leaf area volume density [see (1)].

B. Implications for LAI Measurement

This study highlighted the necessity of accounting for the topographic effect on LAI measurement. The satisfactory performance of PLC on LAI estimation for continuous canopy over mountainous regions has been demonstrated in [3] and [25] by computer simulation. However, its performance for discrete canopy has not yet been quantitatively analyzed. For example, Luisa *et al.* [3] found that the estimated LAI after PLC was lower than that without correction, conflicting with the underestimation phenomenon caused by topography. This study systematically quantified the performance of PLC for discrete canopy by computer simulation, addressing the lack of sufficient *in situ* measurements over mountainous regions which hinder the assessment of the LAI estimation method. The gain in LAI estimation accuracy for discrete canopy is first given. It was found that, after PLC the topography-induced

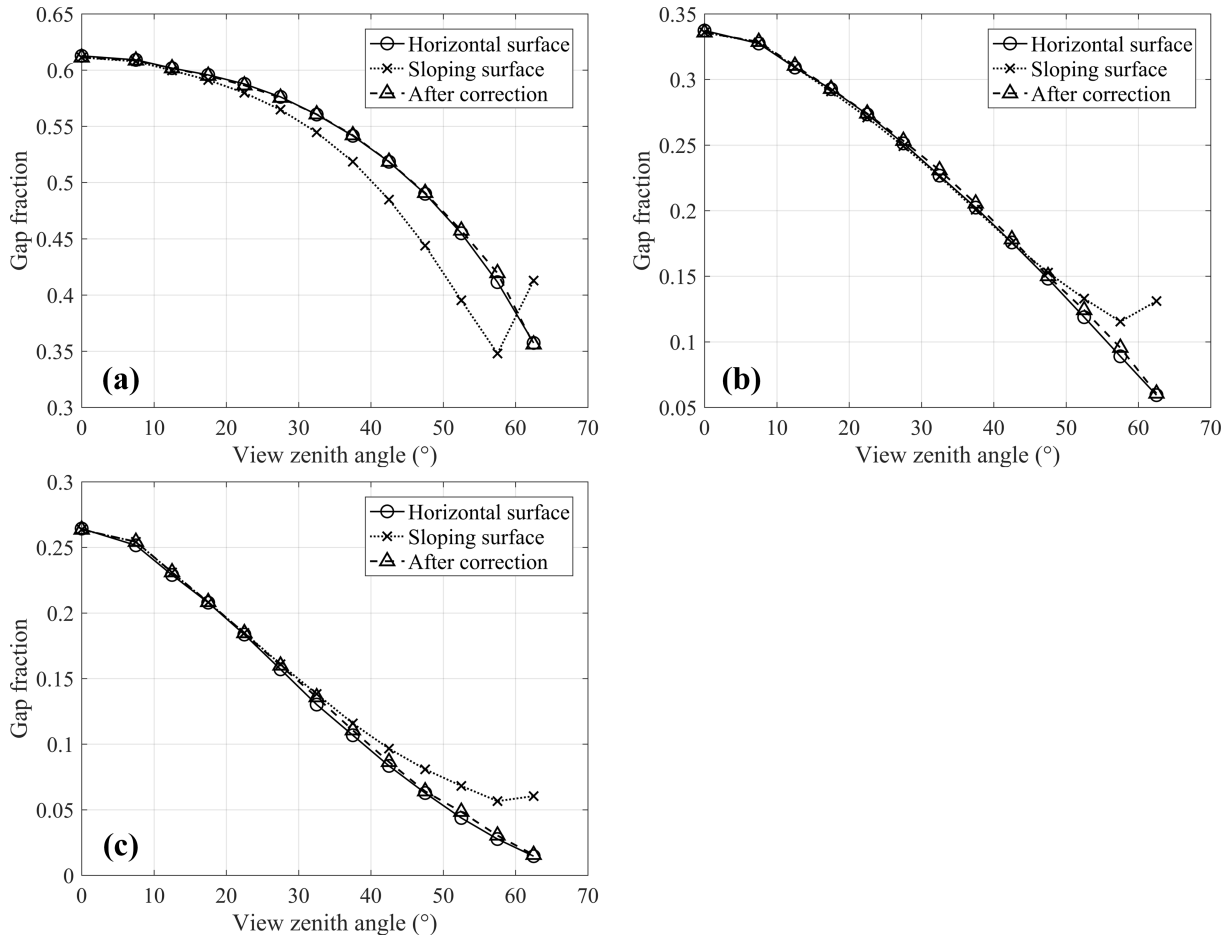

Fig. 12. Azimuthally averaged gap fraction versus view zenith angle for a dense forest with FCC of 74%. The leaf inclination angle distribution was spherical, and the slope was set as 30° for sloping surface. LAIs were set as (a) 1, (b) 3, and (c) 5, respectively.

uncertainty can be reduced to less than 7.3% even for the very low FCC canopy with significant clumping.

The selection of zenith angle influences the *in situ* LAI estimation [51]. Too slant gap fraction was commonly avoided to reduce the influence of diffuse scattering and other factors [43]. Sensitivity analysis found that topography imposes a slight influence on the gap fraction in the small zenith, e.g., <30° (see Figs. 8 and 12). Therefore, the gap fraction measured within the zenith angle of nadir to 30° is recommended for minimizing the topographic effect. An interesting angle for the gap fraction measurement is the zenith of 57.5°, in which the gap fraction exhibits independence from leaf angle distribution [52]. Although this special zenith angle is commonly used, we found that it is very sensitive to the slope (see Figs. 8 and 12). When applied to mountainous regions, this zenith angle should be used with caution and PLC should be employed to mitigate topography effect.

Although PLC can reconstruct the horizontally equivalent gap fraction, the information embedded in the angular section within the topographic mask, up-slope areas blocked by sloping surface, is totally lost (see Figs. 7 and 11). However, this information lost would not influence the reconstruction of the azimuthally average gap fraction (see Figs. 8 and 12) and would not propagate to the estimated LAI. Therefore, the abandonment of the topographic mask is recommended rather than setting its gap fraction to zero [3], [26]. Compared with field campaign over the horizontal surface, additional measurements should be collected over mountainous regions. For example, the alignment of the image with compass and bubble level, and the recording of the slope and aspect of the sloping surface is required for the proper delineation of the topographic mask.

In this study, the topographic effect on LAI measurement and the performance of PLC were specifically analyzed assuming that the clumping information of canopy, e.g., crown shape and distribution, was given. However, the clumping properties are also unknown in reality and interact with the topographic effect [4]. Therefore, topographic and clumping effects should be simultaneously addressed in LAI measurement for forest over mountainous regions. Hu *et al.* [29] demonstrated that path length distribution contains clumping information. The frequency distribution of the path length for the simulated dense forest is shown in Fig. 15. As expected, the distributions for sloping surfaces are quite different from the one for a horizontal surface, except for the case when the surface aspect is perpendicular to the observation azimuth (aspect = 90, in this simulation). This study further confirms that the clumping and topographic effects correlated with each other. Considering that clumping and topographic effects can be accounted for by path length distribution [29] and PLC, it may be possible to develop a uniform framework to cope with topographic and clumping

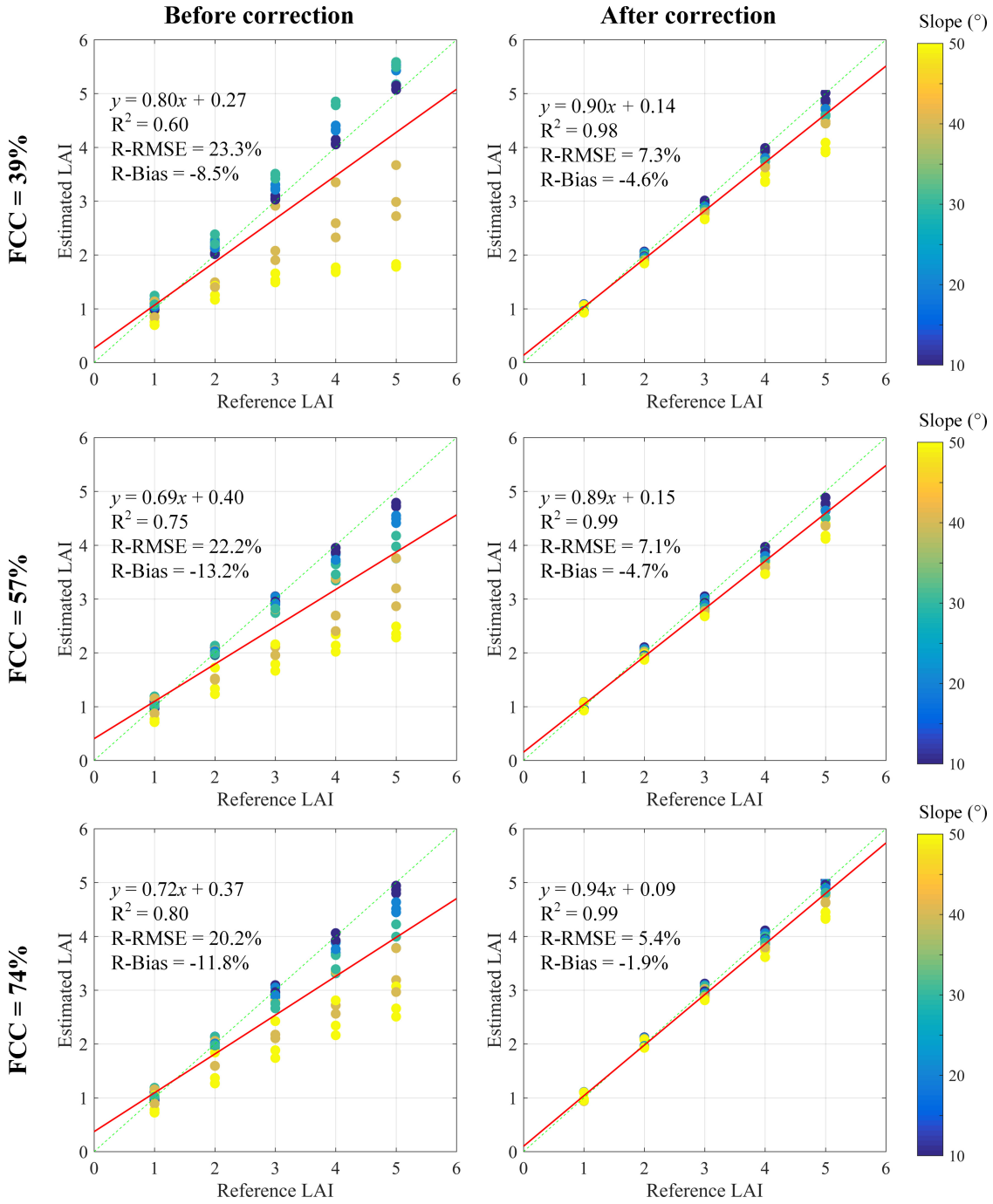

Fig. 13. Comparisons between the reference LAI and the estimated LAI from LUT for different FCCs before and after PLC. The canopies are assumed to be discrete and overlaid sloping surfaces during the simulation.

effects simultaneously. This physically consistent framework will be developed in our future work.

The topographic variables (i.e., slope and aspect) can also be added in the LUT to account for the topographic effect on LAI estimation explicitly. Yet, this topography-explicit LUT was not adopted in this study. Otherwise, We constructed LUTs only for the horizontal surface. This treatment makes the existing LAI estimation algorithms and software, e.g., CAN_EYE [16] and CIMES [33], usable even for sloping surfaces, given the reconstructed horizontally equivalent gap fraction.

It is also noteworthy that the PLC method was derived based on the continuous canopy assumption. Yet, the analysis revealed that it can be safely applied to discrete canopies. This can be explained by the "effective parameters" paradigm, i.e., a 1-D model can mimic the features of a 3-D canopy if the effective parameters were used rather than the true ones [53]. Specifically, for LAI, the effective value can be estimated by multiplying the true value by clumping index [54]. This study confirmed the validity of the "effective parameters" paradigm in topographic correction for the gap fraction.

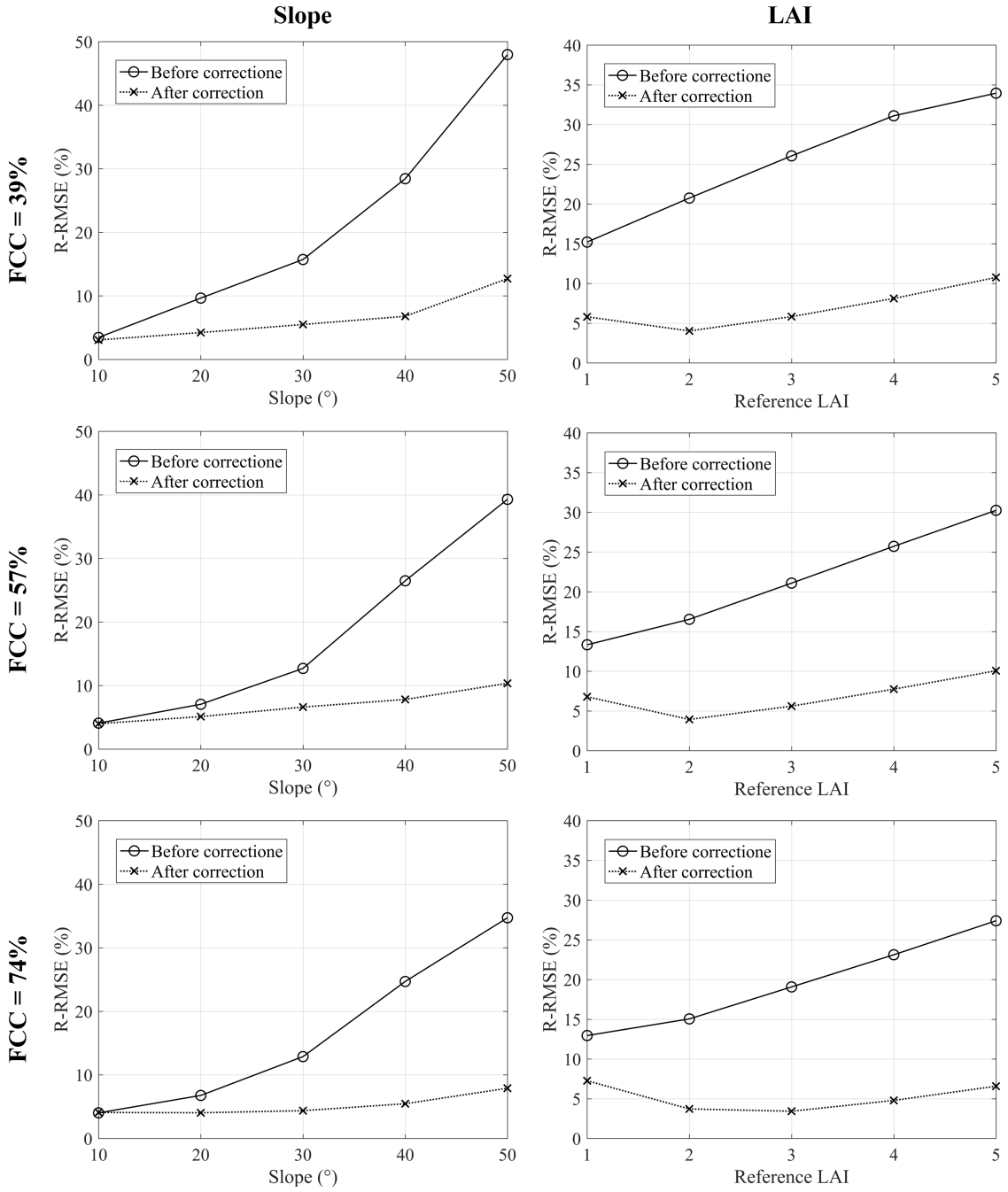

Fig. 14. Variation of LAI estimation uncertainty (represented by R-RMSE) with slope and reference LAI for discrete forest canopy.

This study deduced the transformation relationship between the gap fraction over the sloping surface and its horizontally equivalent value. Based on PLC, the LAI over sloping surface can also be directly transferred to horizontally equivalent LAI. This will significantly improve existing LAI products which generally neglect topographic influences in their retrieval algorithms. The "LAI-level" transformation will be tested in our future work.

C. Computer Simulation and Embedded Uncertainties

This study analyzed the topographic effect and the rationality of PLC on LAI measurement by computer simulation. This simulation method overcomes the problem of lacking sufficient and detailed *in situ* measurements.

The topographic effect and PLC performance for homogeneous canopy were assessed using CANOPIX software [5]. CANOPIX is an easy-to-use tool dedicatedly designed for generating HP for continuous canopy under varying structure properties and terrains [7]. However, it cannot apply to discrete canopy, so a ray-tracing framework was proposed for the discrete cases. Note that the computer simulation method was also widely used in other studies related to the assessment of LAI measurement methods. Most of the studies directly relied on existing simulation software. For example, Cao *et al.* [25], Leblanc and Fournier [35], and Woodgate *et al.* [36], employed RAPID [55], POV-Ray (www.povray.org) and librat [56], respectively. Although these software are all relatively mature and performed satisfactorily in HP simulation,

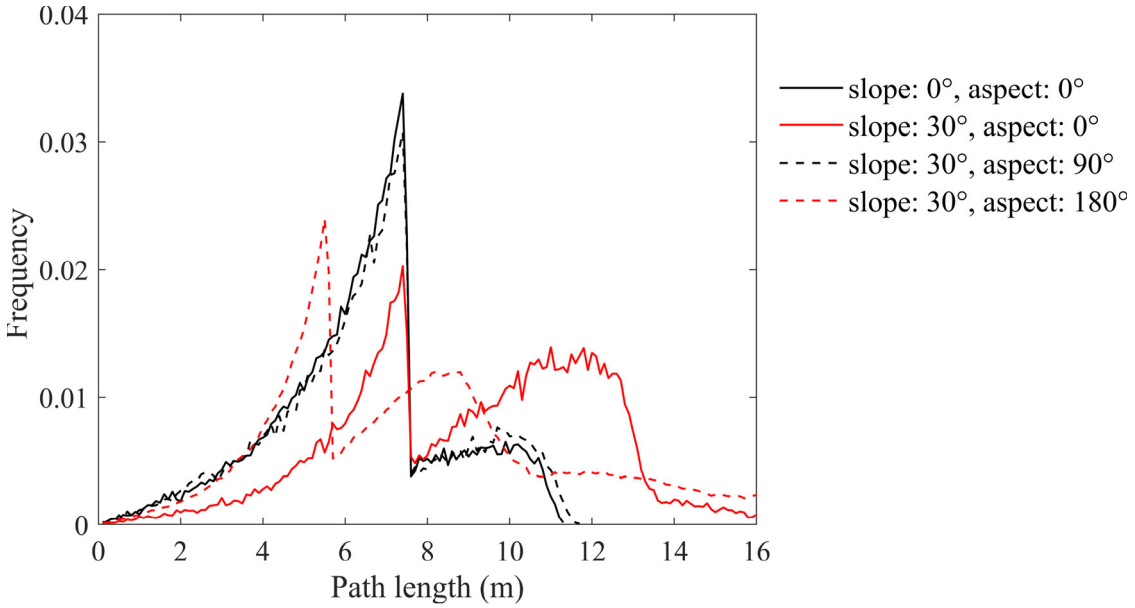

Fig. 15. Frequenc distribution of path length for an identical dense forest (with an FCC of 74%) with different surface orientations. The observation zenith and azimuth angles were set as 30° and 0°, respectively.

they cannot generate path length, hindering the direct analysis of topography-induced path length distortion. This drawback was fully solved in our simulation framework, and the path length distribution for the discrete canopy can be generated as an intermediate outcome (Figs. 5 and 15).

We acknowledge that several factors may influence the credibility of the assessment results.

First, the topographic and clumping effects were separately considered. For example, three respective LUTs were constructed for the forestry scenes (Fig. 4). This may overestimate the retrieval accuracy of the LUT method for forest. In other words, the derived topography-induced uncertainty for forest (20%) only accounts for the first-order effect, and the high order interaction between the clumping and topographic effects was neglected [57], i.e., this may underestimate the total topography-induced uncertainty.

Second, the assessment results in this study are from the most commonly used LAI estimation method, i.e., LUT driven by multiangular gap fraction. Other estimation methods, e.g., those based on the zenith of 57.5° [7], [52] are also worth testing to give a more comprehensive result.

Third, this study defined LAI relative to horizontal surfaces. In few studies, LAI was recommended to be defined over sloping surfaces [2]. However, this is not a big problem as the former definition can be easily transferred to the latter one through multiplying by the cosine of the slope.

Fourth, the surface was assumed to be totally sloped, and the fluctuation within the slope was neglected. The subpixel scale topographic effect, also known as composite sloping terrain [58], exerts influence on the radiative transfer process [39], [59]. However, LAI field measurement is often conducted at a relatively small scale. For example, the essential sampling unit for LAI product validation activity is recommended to be around 30 m × 30 m [60]. At such a small scale the subpixel scale topographic effect would not incur too much uncertainty.

Moreover, other methods to calculate path length exist in the literature, e.g., that proposed by Frazer *et al.* [28]. However, our previous study demonstrated that the selection of path length parameterization has a negligible influence on topographic correction [32].

Finally, branches, twigs, and other nonphotosynthetic organizations were neglected during our simulation. Piayda *et al.* [61] reported that the neglect of woody tissue could yield uncertainty about 6.9%. In addition, the tree envelope was abstracted as a spheroid, and the trees were assumed to be randomly located. Yet different tree shapes and spatial distributions exist in reality. A more realistic representation of forest is needed to further confirm our assessment results.

VI. Conclusion

A computer simulation framework was proposed to assess the topographic effect and the performance of PLC on LAI measurements over sloping terrains. The simulation was achieved using CANOPIX software [5] and a dedicatedly designed ray-tracing method for continuous and discrete canopies, respectively. We produced virtual gap fraction covering a broad range of canopy structures and the following three main conclusions were drawn.

1) Computer simulation is an effective tool in the assessment of PLC for the topographic effect suppression: Computer simulation can be employed to assess both the intermediate variables of the LAI estimation process (e.g., horizontally equivalent gap fraction and azimuthally averaged gap fraction) and the final LAI estimation accuracy.
2) Topographic correction should be specially considered for LAI measurements over mountainous regions: Simulations found that the topography-induced uncertainty in LAI measurements is around 14.3% and more than 20% for continuous and discrete canopies, respec-

tively. And the topographic effect is influenced by FCC, and the largest uncertainty which corresponds to extensively clumping canopy can research to nearly 50%.

3) PLC can significantly improve LAI measurements over sloping terrains: the topography-induced uncertainty can be reduced to 1.8% and less than 7.3%, respectively, for continuous and discrete canopies, after PLC, meeting the up-to-date uncertainty threshold established by the GCOS (15%). The simulation results of this study can inform the design of the protocol for LAI measurements over mountainous regions and can be further improved to add more realistic simulation.

REFERENCES

[1] J. M. Chen and T. A. Black, "Defining leaf area index for non-flat leaves," *Plant Cell Environ.*, vol. 15, no. 4, pp. 421–429, May 1992.

[2] F. Baret *et al.*, "Global leaf area index product validation good practices," CEOS, Tech. Rep. V2.0, 2014.

[3] E. María Luisa, B. Frédéric, and W. Marie, "Slope correction for LAI estimation from gap fraction measurements," *Agricult. Forest Meteorol.*, vol. 148, no. 10, pp. 1553–1562, Sep. 2008.

[4] F. Montes, P. Pita, A. Rubio, and I. Canellas, "Leaf area index estimation in mountain even-aged Pinus silvestris L. Stands from hemispherical photographs," *Agricult. Forest Meteorol.*, vol. 145, nos. 3–4, pp. 215–228, Aug. 2007.

[5] P. Schleppi, M. Conedera, I. Sedivy, and A. Thimonier, "Correcting non-linearity and slope effects in the estimation of the leaf area index of forests from hemispherical photographs," *Agricult. Forest Meteorol.*, vol. 144, nos. 3–4, pp. 236–242, Jun. 2007.

[6] G. B. Bonan and S. C. Doney, "Climate, ecosystems, and planetary futures: The challenge to predict life in Earth system models," *Science*, vol. 359, no. 6375, Feb. 2018, Art. no. eaam8328.

[7] A. Gonsamo, J.-M. Walter, J. M. Chen, P. Pellikka, and P. Schleppi, "A robust leaf area index algorithm accounting for the expected errors in gap fraction observations," *Agricult. Forest Meteorol.*, vol. 248, pp. 197–204, Jan. 2018.

[8] J. Huang *et al.*, "Evaluation of regional estimates of winter wheat yield by assimilating three remotely sensed reflectance datasets into the coupled WOFOST–PROSAIL model," *Eur. J. Agronomy*, vol. 102, pp. 1–13, Jan. 2019.

[9] C. Jiang, Y. Ryu, H. Fang, R. Myneni, M. Claverie, and Z. Zhu, "Inconsistencies of interannual variability and trends in long-term satellite leaf area index products," *Glob Change Biol.*, vol. 23, no. 10, pp. 4133–4146, Oct. 2017.

[10] K. Yan *et al.*, "Evaluation of MODIS LAI/FPAR product collection 6. Part 2: Validation and intercomparison," *Remote Sens.*, vol. 8, no. 6, p. 460, May 2016.

[11] I. Jonckheere *et al.*, "Review of methods for *in situ* leaf area index determination: Part I. Theories, sensors and hemispherical photography," *Agricult. Forest Meteorol.*, vol. 121, nos. 1–2, pp. 19–35, Jan. 2004.

[12] X. Mu *et al.*, "Evaluation of sampling methods for validation of remotely sensed fractional vegetation cover," *Remote Sens.*, vol. 7, no. 12, pp. 16164–16182, Dec. 2015.

[13] Y. Zeng *et al.*, "Extracting leaf area index by sunlit foliage component from downward-looking digital photography under clear-sky conditions," *Remote Sens.*, vol. 7, no. 10, pp. 13410–13435, Oct. 2015.

[14] Y. Zeng *et al.*, "A sampling strategy for remotely sensed LAI product validation over heterogeneous land surfaces," *IEEE J. Sel. Top. Appl. Earth Observ. Remote Sens.*, vol. 7, no. 7, pp. 3128–3142, Jul. 2014.

[15] J. M. Chen, "Optically-based methods for measuring seasonal variation of leaf area index in boreal conifer stands," *Agricult. Forest Meteorol.*, vol. 80, nos. 2–4, pp. 135–163, Jul. 1996.

[16] V. Demarez, S. Duthoit, F. Baret, M. Weiss, and G. Dedieu, "Estimation of leaf area and clumping indexes of crops with hemispherical photographs," *Agricult. Forest Meteorol.*, vol. 148, no. 4, pp. 644–655, Apr. 2008.

[17] H. Fang, W. Li, S. Wei, and C. Jiang, "Seasonal variation of leaf area index (LAI) over paddy rice fields in NE China: Intercomparison of destructive sampling, LAI-2200, digital hemispherical photography (DHP), and AccuPAR methods," *Agricult. Forest Meteorol.*, vols. 198–199, pp. 126–141, Nov. 2014.

[18] Y. Qu *et al.*, "LAINet–A wireless sensor network for coniferous forest leaf area index measurement: Design, algorithm and validation," *Comput. Electron. Agricult.*, vol. 108, pp. 200–208, Oct. 2014.

[19] G. Yin *et al.*, "Derivation of temporally continuous LAI reference maps through combining the LAINet observation system with CACAO," *Agricult. Forest Meteorol.*, vol. 233, pp. 209–221, Feb. 2017.

[20] Y. Zeng *et al.*, "An optimal sampling design for observing and validating long-term leaf area index with temporal variations in spatial heterogeneities," *Remote Sens.*, vol. 7, no. 2, pp. 1300–1319, Jan. 2015.

[21] Y. Ryu, G. Lee, S. Jeon, Y. Song, and H. Kimm, "Monitoring multilayer canopy spring phenology of temperate deciduous and evergreen forests using low-cost spectral sensors," *Remote Sens. Environ.*, vol. 149, pp. 227–238, Jun. 2014.

[22] D. Raymaekers *et al.*, "Spot-vegetation GEOV1 biophysical parameters in semi-arid agro-ecosystems," *Int. J. Remote Sens.*, vol. 35, no. 7, pp. 2534–2547, Apr. 2014.

[23] M. Campos-Taberner *et al.*, "Multitemporal monitoring of plant area index in the valencia rice district with PocketLAI," *Remote Sens.*, vol. 8, no. 3, p. 202, Mar. 2016.

[24] Y. Qu, J. Wang, J. Song, and J. Wang, "Potential and limits of retrieving conifer leaf area index using smartphone-based method," *Forests*, vol. 8, no. 6, p. 217, Jun. 2017.

[25] B. Cao *et al.*, "Comparison of five slope correction methods for leaf area index estimation from hemispherical photography," *IEEE Geosci. Remote Sens. Lett.*, vol. 12, no. 9, pp. 1958–1962, Sep. 2015.

[26] A. Gonsamo and P. Pellikka, "Methodology comparison for slope correction in canopy leaf area index estimation using hemispherical photography," *Forest Ecol. Manage.*, vol. 256, no. 4, pp. 749–759, Aug. 2008.

[27] J.-M.-N. Walter and E. F. Torquebiau, "The computation of forest leaf area index on slope using fish-eye sensors," *Comp. Rendus Acad. Sci. III, Sci. Vie*, vol. 323, no. 9, pp. 801–813, Sep. 2000.

[28] G. Frazer, J. A. Trofymow, and K. P. Lertzman, "A method for estimating canopy openness, effective leaf area index, and photosynthetically active photon flux density using hemispherical photography and computerized image analysis techniques," Pacific Forestry Centre, Victoria, BC, Canada, Tech. Rep., 1997, p. 73.

[29] R. Hu, G. Yan, X. Mu, and J. Luo, "Indirect measurement of leaf area index on the basis of path length distribution," *Remote Sens. Environ.*, vol. 155, pp. 239–247, Dec. 2014.

[30] G. Yin, A. Li, W. Zhao, H. Jin, J. Bian, and S. Wu, "Modeling canopy reflectance over sloping terrain based on path length correction," *IEEE Trans. Geosci. Remote Sens.*, vol. 55, no. 8, pp. 4597–4609, Aug. 2017.

[31] R. Duursma, J. Marshall, and A. Robinson, "Leaf area index inferred from solar beam transmission in mixed conifer forests on complex terrain," *Agricult. Forest Meteorol.*, vol. 118, nos. 3–4, pp. 221–236, Sep. 2003.

[32] G. Yin *et al.*, "PLC: A simple and semi-physical topographic correction method for vegetation canopies based on path length correction," *Remote Sens. Environ.*, vol. 215, pp. 184–198, Sep. 2018.

[33] A. Gonsamo, J.-M.-N. Walter, and P. Pellikka, "CIMES: A package of programs for determining canopy geometry and solar radiation regimes through hemispherical photographs," *Comput. Electron. Agricult.*, vol. 79, no. 2, pp. 207–215, Nov. 2011.

[34] Y. Chen *et al.*, "Estimation of forest leaf area index using terrestrial laser scanning data and path length distribution model in open-canopy forests," *Agricult. Forest Meteorol.*, vol. 263, pp. 323–333, Dec. 2018.

[35] S. Leblanc and R. Fournier, "Hemispherical photography simulations with an architectural model to assess retrieval of leaf area index," *Agricult. Forest Meteorol.*, vol. 194, pp. 64–76, Aug. 2014.

[36] W. Woodgate *et al.*, "Quantifying the impact of woody material on leaf area index estimation from hemispherical photography using 3D canopy simulations," *Agricult. Forest Meteorol.*, vols. 226–227, pp. 1–12, Oct. 2016.

[37] S. G. Leblanc, J. M. Chen, R. Fernandes, D. W. Deering, and A. Conley, "Methodology comparison for canopy structure parameters extraction from digital hemispherical photography in boreal forests," *Agricult. Forest Meteorol.*, vol. 129, nos. 3–4, pp. 187–207, Apr. 2005.

[38] J. Pisek, M. Lang, T. Nilson, L. Korhonen, and H. Karu, "Comparison of methods for measuring gap size distribution and canopy nonrandomness at Jarvselja RAMI (radiation transfer model intercomparison) test sites," *Agricult. Forest Meteorol.*, vol. 151, no. 3, pp. 365–377, Mar. 2011.

[39] J. Wen *et al.*, "Characterizing land surface anisotropic reflectance over rugged terrain: A review of concepts and recent developments," *Remote Sens.*, vol. 10, no. 3, p. 370, Feb. 2018.
[40] J. Geng *et al.*, "Influence of the exclusion distance among trees on gap fraction and foliage clumping index of forest plantations," *Trees*, vol. 30, no. 5, pp. 1683–1693, Oct. 2016.
[41] P. North, "Three-dimensional forest light interaction model using a Monte Carlo method," *IEEE Trans. Geosci. Remote Sens.*, vol. 34, no. 4, pp. 946–956, Jul. 1996.
[42] G. Yan *et al.*, "Scale effect in indirect measurement of leaf area index," *IEEE Trans. Geosci. Remote Sens.*, vol. 54, no. 6, pp. 3475–3484, Jun. 2016.
[43] M. Lang, T. Nilson, A. Kuusk, J. Pisek, L. Korhonen, and V. Uri, "Digital photography for tracking the phenology of an evergreen conifer stand," *Agricult. Forest Meteorol.*, vol. 246, pp. 15–21, Nov. 2017.
[44] J. Verrelst, J. P. Rivera, G. Leonenko, L. Alonso, and J. Moreno, "Optimizing LUT-based RTM inversion for semiautomatic mapping of crop biophysical parameters from Sentinel-2 and -3 data: Role of cost functions," *IEEE Trans. Geosci. Remote Sens.*, vol. 52, no. 1, pp. 257–269, Jan. 2014.
[45] B. Xu *et al.*, "An integrated method for validating long-term leaf area index products using global networks of site-based measurements," *Remote Sens. Environ.*, vol. 209, pp. 134–151, May 2018.
[46] M. Weiss, F. Baret, G. Smith, I. Jonckheere, and P. Coppin, "Review of methods for *in situ* leaf area index (LAI) determination," *Agricult. Forest Meteorol.*, vol. 121, nos. 1–2, pp. 37–53, Jan. 2004.
[47] *The Global Observing System for Climate: Implementation Needs*, GCOS, 2016.
[48] J. Heiskanen *et al.*, "Seasonal variation in MODIS LAI for a boreal forest area in Finland," *Remote Sens. Environ.*, vol. 126, pp. 104–115, Nov. 2012.
[49] A. D. Richardson, D. B. Dail, and D. Hollinger, "Leaf area index uncertainty estimates for model–data fusion applications," *Agricult. Forest Meteorol.*, vol. 151, no. 9, pp. 1287–1292, Sep. 2011.
[50] Y. Ryu, T. Nilson, H. Kobayashi, O. Sonnentag, B. E. Law, and D. D. Baldocchi, "On the correct estimation of effective leaf area index: Does it reveal information on clumping effects?" *Agricult. Forest Meteorol.*, vol. 150, no. 3, pp. 463–472, Mar. 2010.
[51] S. G. Leblanc and J. M. Chen, "A practical scheme for correcting multiple scattering effects on optical LAI measurements," *Agricult. Forest Meteorology*, vol. 110, no. 2, pp. 125–139, Dec. 2001.
[52] F. Baret, B. De Solan, R. Lopez-Lozano, K. Ma, and M. Weiss, "GAI estimates of row crops from downward looking digital photos taken perpendicular to rows at 57.5° zenith angle: Theoretical considerations based on 3D architecture models and application to wheat crops," *Agricult. Forest Meteorol.*, vol. 150, no. 11, pp. 1393–1401, Oct. 2010.
[53] J.-L. Widlowski, B. Pinty, T. Lavergne, M. Verstraete, and N. Gobron, "Using 1-D models to interpret the reflectance anisotropy of 3-D canopy targets: Issues and caveats," *IEEE Trans. Geosci. Remote Sens.*, vol. 43, no. 9, pp. 2008–2017, Sep. 2005.
[54] B. Pinty *et al.*, "Exploiting the MODIS albedos with the two-stream inversion package (JRC-TIP): 1. Effective leaf area index, vegetation, and soil properties," *J. Geophys. Res.*, vol. 116, no. D9, May 2011.
[55] H. Huang, W. Qin, and Q. Liu, "RAPID: A radiosity applicable to porous individual objects for directional reflectance over complex vegetated scenes," *Remote Sens. Environ.*, vol. 132, pp. 221–237, May 2013.
[56] P. Lewis, "Three-dimensional plant modelling for remote sensing simulation studies using the botanical plant modelling system," *Agronomie*, vol. 19, nos. 3–4, pp. 185–210, 1999.
[57] A. Saltelli, M. Ratto, S. Tarantola, and F. Campolongo, "Sensitivity analysis practices: Strategies for model-based inference," *Rel. Eng. Syst. Saf.*, vol. 91, nos. 10–11, pp. 1109–1125, Oct. 2006.
[58] D. Hao *et al.*, "Modeling anisotropic reflectance over composite sloping terrain," *IEEE Trans. Geosci. Remote Sens.*, vol. 56, no. 7, pp. 3903–3923, Jul. 2018.
[59] J. Wen, Q. Liu, Q. Liu, Q. Xiao, and X. Li, "Scale effect and scale correction of land-surface albedo in rugged terrain," *Int. J. Remote Sens.*, vol. 30, no. 20, pp. 5397–5420, Sep. 2009.
[60] J. Morisette *et al.*, "Validation of global moderate-resolution LAI products: A framework proposed within the CEOS land product validation subgroup," *IEEE Trans. Geosci. Remote Sens.*, vol. 44, no. 7, pp. 1804–1817, Jul. 2006.
[61] A. Piayda, M. Dubbert, C. Werner, A. Vaz Correia, J. S. Pereira, and M. Cuntz, "Influence of woody tissue and leaf clumping on vertically resolved leaf area index and angular gap probability estimates," *Forest Ecol. Manage.*, vol. 340, pp. 103–113, Mar. 2015.

Gaofei Yin received the Ph.D. degree from the Institute of Remote Sensing and Digital Earth, Chinese Academy of Sciences, Beijing, China, in 2015.

From 2015 to 2018, he was with the Institute of Mountain Hazards and Environment, Chinese Academy of Sciences, Chengdu, China. Since 2018, he has been an Associate Professor with the Faculty of Geosciences and Environmental Engineering, Southwest Jiaotong University, Chengdu. He is currently a Marie Skłodowska-Curie Individual Fellow with the Global Ecology Unit, Center for Ecological Research and Forestry Applications, Barcelona, Spain. His research interests include canopy reflectance modeling, biophysical variables estimation, and climate-vegetation dynamics.

Biao Cao received the B.Sc. degree in geographic information system from Beijing Forestry University, Beijing, China, in 2009, and the Ph.D. degree in cartography and geographic information system from the Institute of Remote Sensing and Digital Earth, Chinese Academy of Sciences (CAS), Beijing, in 2014.

From December 2017 to December 2018, he was a Visiting Scientist with the DART Group, CESBIO (CNRS, UPS, CNES, IRD, INRA), Toulouse, France. He is currently an Associate Professor with the State Key Laboratory of Remote Sensing Science, Institute of Remote Sensing and Digital Earth, CAS. His research interests include the canopy structure parameter retrieval, thermal radiation transfer modeling, and long-wave upward radiation estimation considering the thermal radiation directionality.

Jing Li received the B.S. degree in geology from Zhejiang University, Hangzhou, China, in 2002, and the Ph.D. degree in cartography and geographic information system from the Graduate University of the Chinese Academy of Sciences (CAS), Beijing, China, in 2007.

She was a Visiting Scholar with Wageningen University, Wageningen, The Netherlands, from 2008 to 2009, and with Plant Functional Biography and Climate Change Cluster, University of Technology Sydney, Ultimo, NSW, Australia, in 2014. She is currently an Associate Professor with the Institute of Remote Sensing and Digital Earth, CAS. Her primary research interests include optical radiative transfer modeling, vegetation parameter inversion methods from remote sensing, agricultural application of remote sensing, and vegetation change detection.

Weiliang Fan received the B.S. degree from Shandong Agricultural University, Tai'an, China, in 2007, the M.S. degree from Zhejiang A & F University, Lin'an, China, in 2010, and the Ph.D. degree from Nanjing University, Nanjing, China, in 2013.

He is currently an Associate Professor with Zhejiang A & F University. His major research interest is in the remote sensing of vegetation.

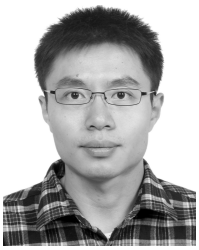

Yelu Zeng received the B.S. degree in remote sensing from Wuhan University, Wuhan, China, in 2011, and the Ph.D. degree from the Institute of Remote Sensing and Digital Earth, Chinese Academy of Sciences, Beijing, China, in 2016.

He is currently a Post-Doctoral Fellow with the Carnegie Institution for Science, Stanford, CA, USA. His research interests include 3-D radiative transfer modeling over vegetation canopies and solar-induced chlorophyll fluorescence (SIF).

Baodong Xu received the Ph.D. degree from the Institute of Remote Sensing and Digital Earth, Chinese Academy of Sciences, Beijing, China, in 2018.

Since 2018, he has been an Associate Professor with the Macro Agriculture Research Institute, College of Resource and Environment, Huazhong Agricultural University, Wuhan, China. His research interests include biophysical variables estimation, validation of remote sensing products, and remote sensing applications in agriculture.

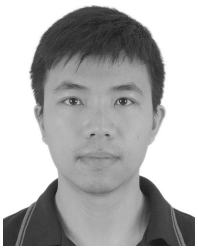

Wei Zhao received the B.S. degree in geographic information system from Beijing Normal University, Beijing, China, in 2006, and the Ph.D. degree in cartography and geographic information system from the Institute of Geographic Sciences and Natural Resources Research, Chinese Academy of Sciences (CAS), Beijing, in 2012.

From 2012 to 2015, he was a Research Assistant with the Institute of Mountain Hazards and Environment (IMHE), CAS, Chengdu, China, where he is currently an Associate Professor. His research field is mountain quantitative remote sensing with special focuses on land surface energy fluxes and soil moisture estimation, spatial scale effect on remote sensing data, terrain effect correction, and thermal environment monitoring.